

Fatigue degradation in the vicinity of contact interface under fretting conditions

Jiří Kuželka,¹ Hynek Chlup,² Josef Jurenka,³ Miroslav Španiel⁴

Abstract: In this paper the current knowledge concerning fretting fatigue damage are briefly summarised and factors with major influence are discussed. Experimental equipment for fretting fatigue tests is presented. The possibilities of displacement field identification by optical measuring were tested regarding partial slipping of contact surfaces measuring. Preliminary measurements on flat specimens with circular hole were carried out. The displacement field at the vicinity of the hole was captured via DANTEC DYNAMICS Q-450. Programme code Istra4D was employed for displacement field evaluation. The measured displacement fields as well as used speckle patterns were processed by scripts using Matlab code.

Keywords: Fretting, Notch, Digital image correlation

1. Introduction

The most of the construction failures is caused by fatigue on the present. The fatigue can be seen as a continuous and irreversible degradation of material which occurs at microscopic level. From the macroscopic point of view it has quite random character. The use of physical models for fatigue damage prediction that involve its nature is difficult and almost impossible in practice. Phenomenological models that involve only observed relations among the crucial factors for fatigue are purely used.

The fatigue life of a construction can be divided into three stages: crack initiation, crack growth and ultimate ductile failure. The first two mentioned stages represent the main part of fatigue life and can take respectively very different amount of time depending on particular case.

¹ Ing. Jiří Kuželka; Department of Mechanics, Biomechanics and Mechatronics; Faculty of Mechanical engineering; Czech Technical University in Prague; Technická 6, 16607, Prague, Czech Republic

² Ing. Hynek Chlup, Laboratory of cardiovascular Biomechanics; Department of Mechanics, Biomechanics and Mechatronics; Faculty of Mechanical engineering; Czech Technical University in Prague; Technická 6, 16607, Prague, Czech Republic

³ Ing. Josef Jurenka; Department of Mechanics, Biomechanics and Mechatronics; Faculty of Mechanical engineering; Czech Technical University in Prague; Technická 6, 16607, Prague, Czech Republic

⁴ Doc. Ing. Miroslav Španiel, CSc.; Department of Mechanics, Biomechanics and Mechatronics; Faculty of Mechanical engineering; Czech Technical University in Prague; Technická 6, 16607, Prague, Czech Republic

A notch can be generally considered as the location of fatigue crack initiation. The stress concentration (the increase of stress gradient) is a typical characteristic. From this point of view the contact interface between bodies can be treated as a notch. In the case of pure geometrical notch the stress field at its vicinity is determined only by its shape in the contrary of “contact notch”. The fatigue of contacting bodies is determined not only by their geometry but also by tribological conditions of contact interface and by the magnitudes of relative slips of contacting surfaces.

1.1. Factors with main influence on fretting fatigue

The fretting fatigue takes place usually near contact interface of bodies with no relative movements. Only the partial relative slips of contact areas appear. The typical construction joints that are exposed to fretting conditions are: flanges, dovetails, hub-shaft connections, cable stands interface, leaf spring washers, leaf and wound springs, etc.

This type of fatigue is influenced by numerous factors thus it is necessary to restrict oneself on the most influencing ones. There are three essential factors influencing fretting fatigue. The first one is the field of strains and stresses at the vicinity of contact interface which can be analysed both analytically and numerically. The second one is the partial slipping of contact surfaces. Contact conditions can be divided into three ranges regarding magnitudes of partial slips: the stick range with slip magnitudes up to $3\mu\text{m}$, the partial slip range with slip magnitudes between $5 - 50\mu\text{m}$ and gross sliding range with slip magnitudes greater than $100\mu\text{m}$ [1, 2]. It worth to mentioning the dependence of fatigue life on slip magnitude is not monotonic it decreases in range of partial slips. The third crucial factor is the friction or more generally tribological conditions between contact areas. All the three essential factors are coupled and can change during construction life.

1.2. Fretting fatigue damage estimations

Both crack initiation and growth stages are usually considered in the models used for fatigue life estimations. The crack initiation does not need be fatigue limit state so the short sometimes long crack growth stage is governing.

The multiaxial fatigue criteria in connection with critical distance theory [3, 4] are usually used for number of cycles to crack initiation computations. It assumes the physical processes leading to crack initiation takes place in small material volume characterised by length which is considered to be a material property. The summary of these criteria can be found e.g. in [5]. There are also criteria based on energy balance concept [6] requiring relatively huge experimental base. In connection with mentioned concepts is necessary s to consider also the wear of material in particular cases [7, 8].

2. Experimental equipment for fretting fatigue tests

At CTU in Prague has been designed experimental equipment for scheduled fretting fatigue tests. It is based on concept of dog bone specimen pressed by pads during the

test. The advantage of this design consist in possibility to use standard loading machines as well as possibility of easy change of pressing pads leading to differential contact conditions set up. Basic stiffness and stress parameters of the equipment were optimised regarding stress and kinematic conditions between specimen and pads. The FE models simulating the first several cycles of dynamic loading were created and solved for various loadings, pads and stiffness of pads loading mechanism. The contact pressure, tangential stresses and relative slips were analysed in the points of highest accumulated slips in contact interface between specimen and pads. The final design is shown in Fig. 1.

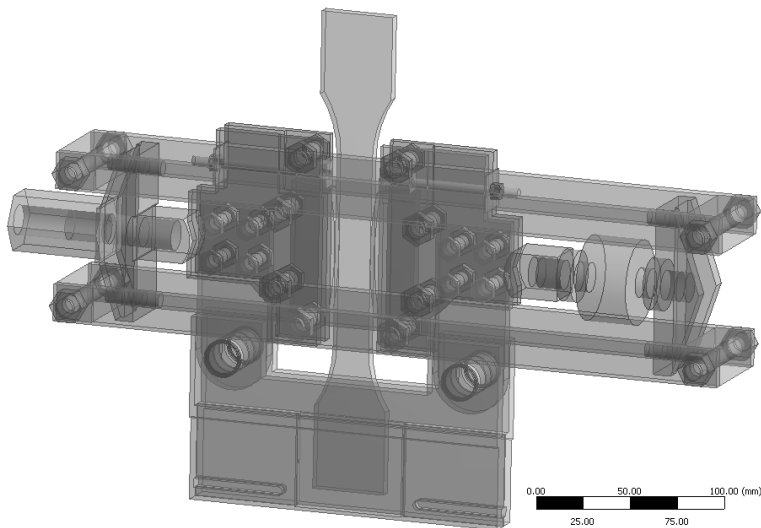


Fig. 1. Design of experimental equipment for fretting fatigue tests.

3. Preliminary measurements

For verification and designing new fretting fatigue criteria it is necessary to base on reliable experimental results. The displacement and strain field measurement at the vicinity of contact interface is quite problematic and is impossible to accomplish it by conventional methods. Some of the optical measuring methods seem to be one of the possible ways to identify these fields. The optical measuring system DANTEC DYNAMICS Q-450 is at disposal at CTU in Prague. It employs digital image correlation method for displacement field estimation [9]. This method is based on correlation of pictures at current and at base state. For a good accuracy of results there is the requirement on stochastic and fine pattern of the measured surface. Since this system has being used for low stiffness specimens exhibiting relatively large deformations the testing is necessary. The use of this system for displacement field measurements of contacting metal specimens is very specific. Really very small displacements need to be measured thus relatively small area must be captured since

the resolution of the camera is only 1Mpix (however very high sampling rates can be used). These facts take special requirements on optics, stochastic speckle pattern and lighting. Employing two cameras in order to measure displacements in all three directions is very limited because of low depth of field caused by special optics. In order to test the system under similar conditions to fretting fatigue tests the flat notched specimens were treated.

3.1. Specimens preparation

Four structural steel specimens Fig. 2. were manufactured by water beam cutting. The surface surrounding the hole was grind with emery paper to achieve appropriate surface quality for speckle pattern coating. The stochastic speckle pattern around the hole has been made by Harder & Steenbeck airbrush. At first the basic white paint had been sprayed and next the black speckles were applied. There were used two different diameters of airbrush nozzle in order to obtain different speckle sizes (signed A and B) and four different speckle densities (signed 1 – 4). Two speckle patterns varying in speckle size were applied on each specimen symmetrically to longitudinal specimen axis. Each pattern differs in speckle density and size as is illustrated in Fig. 3. where one frame is 2.5x2.5 mm. The upper row corresponds to a narrow nozzle and the lower row to the wide one. The columns correspond to different speckle densities.

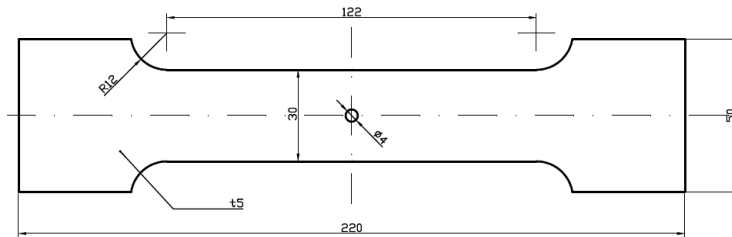


Fig. 2. Geometry of treated specimens.

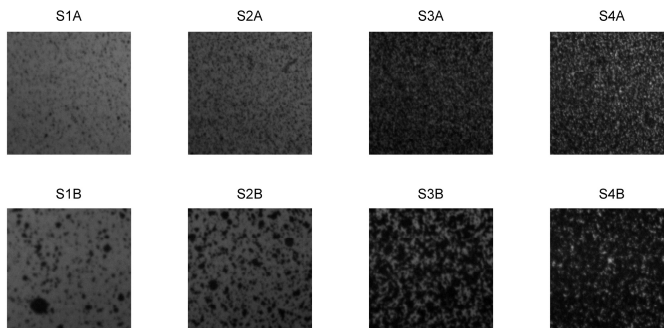


Fig. 3. Tested speckle patterns; size of cell is 2.5x2.5mm; fine pattern in top row; coarse pattern in a bottom row; different speckle densities in columns.

3.2. Arrangement of the experiment

The arrangement of experiment is shown in Fig.3. The specimens were loaded by FPZ tension testing machine. The illumination was provided by two diode lights. The optical chain consists of: objective lens (focal length 105mm and lens opening 1:2.8D) and 2x telekonverter. The size of field of view was approximately 13x10mm. NanoSense MKIII camera with resolution 1260x1024pix was used for picture capturing. For system calibration was used 9x9 chessboard target with cell edge length 1mm.



Fig. 4. Arrangement of the experiment.

The specimens were being loaded monotonically during approximately one minute in range 0 – 8kN corresponding to 0 – 53MPa of nominal stress. During the loading the pictures were being captured with frequency 5Hz as well as analogue data signal corresponding to loading force and displacement of cross bar. The commercial software Istra4D was employed as a control and actuating system.

3.3. Captured data processing

For each specimen were captured 400 pictures. Each picture of actual position as well as analogue signal data was stored in separate files of hdf5 format. At first the force analogue signal was checked and steps where loading took place were selected for digital image correlation process. The speckle size for measured areas A was between 25 – 70 μm (3 – 8pix) and for the areas B was 80 – 240 μm (10 – 30pix).

Table 1. Digital image correlation parameters

	speckle size		grid size		facet size	
	μm	pix	μm	pix	μm	pix
pattern A	25 - 70	3 - 8	80	10	168	21
pattern B	50 - 240	10 - 30	160	20	328	41

The facet (a subset of image used for correlation) and grid (points where displacements are computed) sizes were estimated on the base of mentioned speckle

sizes. The facet size was chosen to be three times bigger than average speckle size for areas A and two times bigger for areas B. The grid size was chosen as half size of facet. The average speckle sizes, grid and facet sizes are summarised in Table 1.

3.4. Results analysis

Two 2D digital image correlations including approximately 300 loading steps were carried out for each specimen; the first for pattern A and the second for pattern B. The computed results (displacements and strains) for each step were exported to hdf5 files and subsequently analysed. The script in Matlab code was written in order to carry out the analysis.

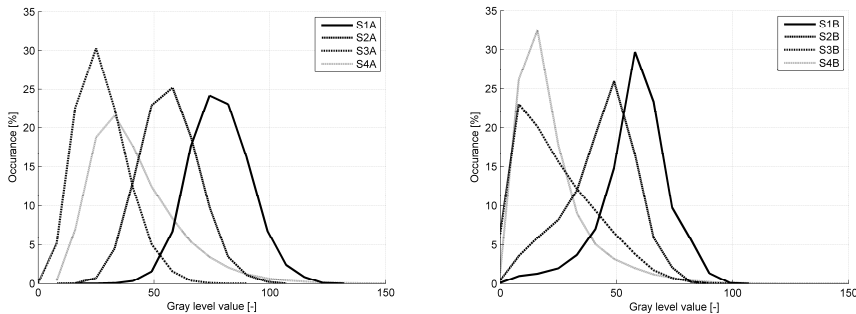


Fig. 5. Histograms of speckle patterns; fine pattern on the left; coarse pattern on the right.

At first the histograms Fig. 5. were extracted from captured images in order to classify the speckle patterns in addition to average speckle size. The displacement fields were analysed next. Eight steps corresponding to 1-8kN applied load were chosen for further analysis of vertical (direction of loading force) displacement field. Since the measured displacement fields were corrupted by noise the computation of deformations directly from this field gives unreasonable results. The smoothing of displacement field can settle this problem. For this procedure was chosen a 9x9 circular disk filter from Matlab filter library. The smoothed displacement fields relative to the centre of hole in vertical direction at 8kN load stage for all evaluated areas are shown in Fig. 6. As relative error measure of smoothing was used the following relation

$$e_v = \frac{\sum_{i=1}^k |v_{mi} - v_{si}|}{\sum_{i=1}^k |v_{si}|} \quad (1)$$

where k is a number of evaluated (grid) points v_{mi} and v_{si} are measured and smoothed displacements in i^{th} point. The error measure dependence on loading force for different speckle patterns is shown in Fig. 6. This error can also be seen as a measure of noise included in the field.

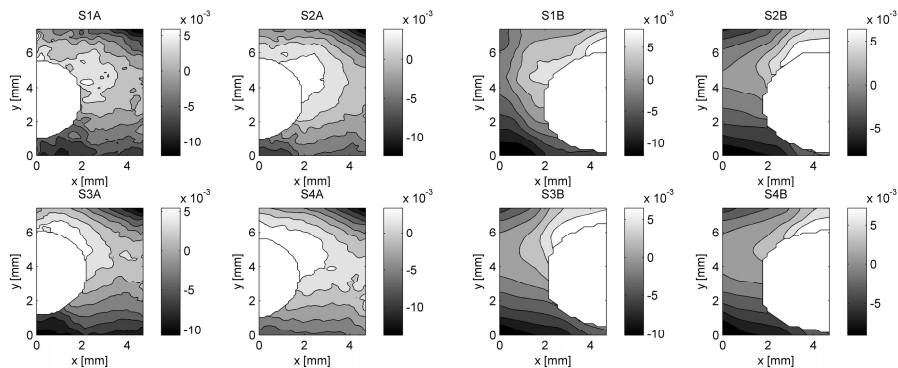


Fig. 5. Horizontal displacement fields relative to centre of hole at 8kN load; fine pattern on the left; coarse pattern on the right.

4. Conclusions

Regarding the speckle patterns the eight types were created. They differ in speckle size Fig.3. and average gray value intensity Fig. 5. The histograms shape differs for A and B patterns. It pointing on fact the finer pattern suffers from low contrast on speckle edges compared to coarse one. In Fig. 6. can be traced the quality of speckle pattern. One can say the noise in measured field decrease as speckle density (and also loading force) increase. One can also see the difference in noise (error) for speckle sizes A and B however it is influenced not only by higher speckle contrast but also by the facet size.

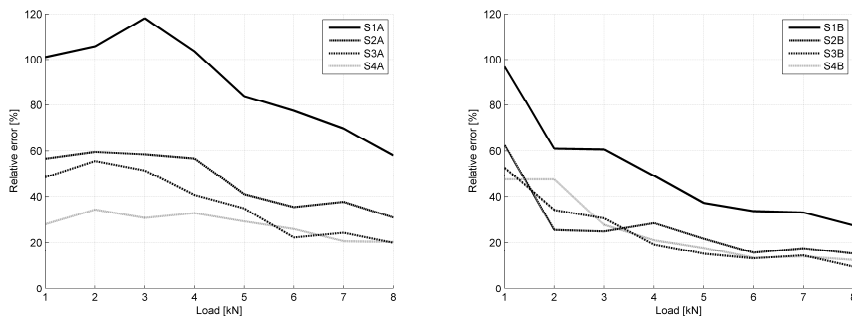


Fig. 6. Relative error of smoothing of displacement field (level of noise) vs. loading force for different speckle patterns densities; fine pattern on the left; coarse pattern on the right.

There is need to be said the contours of smoothed vertical displacement Fig. 5. do not match theoretical results. This discrepancy is probably caused by undesirable loading caused by inappropriate clamping of a specimen thus it was bended in plane perpendicular to sensor plane. The improper grinding of specimens leading to slightly curved surface around the hole could participate on the mismatch too. Nevertheless the measured displacement magnitudes are in the same order as the

theoretical ones. Moreover the range of measured displacements about $20\mu\text{m}$ is sufficient for partial slip measurements during fretting fatigue tests.

Acknowledgements

This work was supported by grant of GACR No. 101/09/1709.

References

- [1] Madge J.J., Leen S.B., McColl I.R. and Shipway P.H., "Contact-evolution based prediction of fretting fatigue life: Effect of slip amplitude," *Wear*, **262**(9-10), pp. 1159–1170 (2007). ISSN 0043-1648.
- [2] Vingsbo O. and Soderberg S., "On fretting wears," *Wear*, **126**(2), pp. 131-147 (1988). ISSN 0043-1648.
- [3] Araujo J.A., Susmel L., Taylor D., Ferro J.C.T. and Mamiya E.N., "On the use of the Theory of Critical Distances and the Modified Wohler Curve Method to estimate fretting fatigue strength of cylindrical contacts," *International Journal of Fatigue*, **29**(1), pp. 95–107 (2007). ISSN 0142-1123.
- [4] Bhattacharya B. and Ellingwood B., "Continuum damage mechanics analysis of fatigue crack initiation," *International Journal of Fatigue*, **20**(9), pp. 631-639 (1998). ISSN 0142-1123.
- [5] Navarro C., Munoz S. and Domínguez J., "On the use of multiaxial fatigue criteria for fretting fatigue life assessment," *International Journal of Fatigue*, **30**(1), pp. 32-44 (2008). ISSN 0142-1123.
- [6] Vidner J. and Leidich E., "Enhanced Ruitz criterion for the evaluation of crack initiation in contact subjected to fretting fatigue," *International Journal of Fatigue*, **29**(9-11), pp. 2040-2049 (2007). ISSN 0142-1123.
- [7] Madge J.J., Leen S.B. and Shipway P.H., "The critical role of fretting wear in the analysis of fretting fatigue," *Wear*, **263**(1-6), pp. 542-551 (2007). ISSN 0043-1648.
- [8] McColl I.R., Ding K. and Leen S.B., "Finite element simulation and experimental validation of fretting wear," *Wear*, **256**(11-12), pp. 1114-1127 (2004). ISSN 0043-1648.
- [9] Sutton A.M., Orteu J. and Schreier W.H., *Image Correlation for Shape, Motion and Deformation Measurements* (Springer, New York, 2009). ISBN 978-0-387-78746-6.